SECTION 102

DETECTION OF OCEAN CHLOROPHYLL FROM EARTH ORBIT

by

Seibert Q. Duntley
Visibility Laboratory
Scripps Institution of Oceanography
University of California, San Diego

Calculations have been made of the magnitude of the optical signature of ocean chlorophyll available to any remote sensor in earth orbit. The study had several goals, and all of them were achieved. First, it was desired to ascertain whether commercially significant concentrations of chlorophyll-A pigments in the ocean would produce a sufficient optical signal at orbital altitudes to operate optical remote sensors, such as those being planned for the Earth Observatory Satellite, on clear and hazy days. Second, it was desired to explore the effect of solar altitude on these optical signals, because this is an important matter in choosing the best orbit for an oceanographic satellite. Third, it was desired to find the best orientation for the field of view for a remote sensor in orbit in order to optimize its ability to detect ocean chlorophyll.

We avoided many uncertainties by using only atmospheric, oceanographic, and lighting data. These were obtained on board ships and from aircraft. The only use we made of mathematical modeling concerned the enrichment of chlorophyll above the concentration found in the ocean water that was measured. Richer waters were simulated by using laboratory spectrophotometric measurements of living cultures of ocean phytoplankton in radiative transfer calculations which predicted the optical properties of ocean waters containing concentrations of chlorophyll-A pigments covering the entire range of commercial importance beginning with arid water, where the concentration is 0.1 mg/m^3 or less, and extending to a concentration of 10 mg/m^3, which characterizes richly productive ocean water.

One of my colleagues at Scripps, John E. Tyler, has a submersible, double-grating, double-channel photoelectric spectroradiometer which he and another colleague, Dr. Raymond C. Smith, have taken on many oceanographic expeditions. Some of their data is recorded in a comparatively new book published by Gordon and Breach, which is entitled "Measurements of Spectral Irradiance Underwater." (1) My first two figures are plotted from tables which begin on page 66 in that volume. These data were obtained in clear, blue, arid ocean water in the southern part of the Gulf of California near Islas Tres Marias. A biologist on board the vessel collected water samples at various depths and measured the concentration of chlorophyll-A pigments by the extraction process; he characterized the water as having a concentration of 0.112 mg/m^3. This ocean location represented, therefore, the upper boundary of commercially arid waters from the standpoint of chlorophyll concentration.

Figure 1 represents the spectral reflectance of deep ocean water as measured beneath the water surface. Figure 2 shows diffuse attenuation coefficients for spectral irradiance in water; they are the slopes of log-linear depth profiles of measured spectral irradiance and are tabulated by Tyler and Smith in their book referenced above. All of our results are based on this pair of spectral curves. Two data are necessary at each wavelength because two independent phenomena, scattering and absorption, govern the spectral properties of water.

From Figures 1 and 2 it was possible to calculate spectral diffuse backscattering coefficients and the spectral diffuse absorption coefficients of the ocean water at Islas Tres Marias by a previously published method. (2) The results are shown in Figures 3 and 4. These coefficients are linearly related to the concentration of chlorophyll-A pigments. Thus, corresponding coefficients for known concentrations of laboratory cultures of ocean phytoplankton can be added to those in Figures 3 and 4 in order to predict the optical properties of ocean water containing any arbitrary concentration of chlorophyll-A pigments.

Our colleagues in marine biology at the Scripps Institution of Oceanography supplied us with laboratory cultures of the most important classes of ocean phytoplankton and measured the concentration of chlorophyll-A pigments in each of them. The collaboration of marine biologist Dale A. Kiefer is very gratefully acknowledged. Together we measured the spectral diffuse reflectance and the spectral diffuse optical density of one centimeter thicknesses of living cultures of typical coccolithophorids, dinoflagelattes, and diatoms. We used the original Hardy recording spectrophotometer for this purpose. (3) Many details of the spectrophotometric technique are in the 1942 paper. (2) The laboratory data are shown in Figures 5 and 6.

Spectral diffuse backscattering coefficients and spectral diffuse absorption coefficients were calculated from Figures 5 and 6 for unit concentrations of each species of phytoplankton, and they are plotted in Figures 7 and 8.

Phytoplankton in commercial fishing grounds are always a mixture of the principal species. We were advised by our colleagues at Scripps who specialize in food-chain marine biology that in commercial fishing grounds the most common mixture contains 12 % coccolithophorids, 38 % dinoflagellates, and 50 % diatoms. Coefficients for the separate cultures were combined in these proportions to produce the curves marked MIXTURE in Figures 7 and 8. The coefficients for that MIXTURE were then added in appropriate concentrations to the corresponding optical coefficients for the arid ocean water measured at Islas Tres Marias. This procedure enabled the spectral reflectance of ocean waters containing chlorophyll-A pigment concentrations from .1 to 10 mg/m^3 to be calculated. Figure 9

illustrates one of these results by means of the curve marked "10 mg/m^3;" the other curve, marked 0.1 mg/m^3, is identical with Figure 1 and represents the measurements of Tyler and Smith at Islas Tres Marias. From the standpoint of ocean color, the curve for 0.1 mg/m^3 depicts blue water, whereas that for 10 mg/m^3 indicates a strong green.

The cholrophyll-A pigments contained in phytoplankton have strong spectral absorption in the blue and in the far red region of the spectrum. The red absorption is probably of little use for remote sensing because the water molecule itself absorbs red light so strongly that daylight does not penetrate deeply. Addition of phytoplankton to arid ocean water causes the reflectance of the ocean to be diminished in the blue region of the spectrum where chlorophyll absorbs strongly. At the same time, however, the reflectance increases in the yellow-green region of the spectrum. This increase in reflectance may seem surprising until it is remembered that ocean phytoplankton both scatter and absorb light. The scattering is due to the fact that they are armored; that is, they have thin cases or shells of calcaceous, silacaceous, or cellulose-like materials. In the blue, absorption due to chlorophyll dominates the optical properties of the phytoplankton, but in the yellowish green (around 560 nm) chlorophyll absorbs very little and scattering predominates. The spectral reflectance of clear ocean water is roughly proportional to the ratio of the spectral back-scattering coefficient to the spectral absorption coefficient.

The way in which the spectral reflectance of ocean water at 450 nm and 560 nm varies with concentration of chlorophyll-A pigments is shown by Figure 10. Interestingly, in terms of green light at 523 nm the ratio of the back-scattering coefficient to absorption coefficient for the mixture of ocean phytoplankton used in this study has the same value as the corresponding ratio of back-scattering to absorption coefficients for the water measured by Tyler and Smith at Islas Tres Marias. Therefore, addition of phytoplankton to this ocean water causes almost no change in the spectral reflectance at 523, although it does diminish the water clarity slightly. This fact causes reflectance curves like those in Figure 9 to exhibit a hinge point at 523 nm.

Having predicted the spectral reflectance characteristics for ocean waters containing the complete range of chlorophyll concentrations that are of importance to ocean food chain productivity it remained to use this information to predict the chlorophyll signal that will reach remote sensors in orbit. Fortunately, my colleagues and I have, for many years, engaged in a data collection program to obtain exactly the type of information that is needed to accomplish this. Our measurements have been made from aircraft, spacecraft, ships, and ground stations. Figures 11 and 12 show the facilities we employed to collect the data that were used in the calculations described in this paper. Figure 11 is a photograph of the specially instrumented C-130 aircraft which is used in the atmospheric

data collection program we conduct under the auspices of the Air Force Cambridge Research Laboratories. This airplane has been extensively modified, both inside and out, for the determination of optical and meteorological parameters. It is equipped, for example, with scanners which map the skies above and below the airplane. At low altitude over the ocean our lower scanner maps the water surface and records the manner in which sunlight and skylight are reflected. All of the optical sensors in the aircraft combine to measure contrast attenuation by the lower atmosphere along any path of sight, inclined upward or downward. This information is supplemented by data taken at sea level with the instrument shown in Figure 12, which we call a contrast reduction meter. It has the capability of determining from a ground station the reduction of contrast throughout the total atmosphere, that is to say, from the surface of the earth to orbital altitude.

The ground based and airborne facilities have been used on hundreds of days in many parts of the world. Our data banks and computer programs for their use were established many years ago and are continually updated. It was a simple matter, therefore, to select measured data representing real days when the path of sight from sea surface to orbit was cloud-free and to combine those data with the ocean reflectance curves in this paper to ascertain the chlorophyll signal available to any orbiting remote sensor.

A typical result is shown in Figure 13. It is a polar plot of the field of view directly beneath an orbiting spacecraft. The nadir is at center. The outer circle represents a circular field of view 50° in angular radius as seen from the spacecraft. On the occasion depicted by this figure, the solar zenith angle was 30.9° and therefore the solar reflection point in the ocean surface is seen 30.9° from the nadir, near the top of the figure on the radial marked zero.

The ocean color sensors planned by NASA for the Earth Observatory Satellite are expected to have a sensitivity sufficient to detect a change in optical input of 0.001 when a sensor element passes from arid water to water containing significant chlorophyll-A pigments. The bold contour in this figure is a locus of points in the field of view where the optical signal changes by 0.001 in passing from arid water to water containing 0.30 mg/m^3 of chlorophyll-A pigments. Within and above this contour the signal level is too small to be detected by the sensor. Throughout the entire remainder of the field of view, however, there is more than enough signal. The figure has been computed for green light at 560 nm and for a surface wind speed of 10 knots, a value below that required to produce whitecaps. The calculation has been based on data for a cloud-free, clear day that was measured in the vicinity of San Diego on 2 September 1964. The air mass was unstable, continental, tropical. The U.S. Weather Bureau reported "visibility" 10 to 20 miles, temperature 72°F to 76°F, relative humidity 0.50 to 0.64. Local meteorologists described it as a "mild Santa Ana condition."

On that day optical data were taken from soon after sunrise until nearly sunset. From our data bank we have selected six solar altitudes ranging from a high solar zenith angle of 24.3° to a low sun with a solar zenith angle of 70.6°. These six solar zenith angles are compared by the curves in Figure 14. They represent orbital signal levels in the plane of the sun for a chlorophyll concentration of 0.30 mg/m^3. The second curve from the top is for the solar zenith angle 30.9° and corresponds with the polar plot in Figure 13. The left point on the curve represents the optical signal available to the sensor at the top of the diagram. It is less than the sensor threshold, 0.001. Progressing to the right, the curve passes through the solar reflection point and climbs to the 0.001 threshold near 11° from the nadir. From there on there is ample signal for the sensor.

Several conclusions can be drawn from Figure 14. The available optical signal was greatest in the case of the curve representing a solar zenith angle of 30.9°. The signal level and its angular extent is almost but not quite as good when the sun is at 24.3°, but it is badly degraded when the solar zenith angle is 42.0°. Virtually none of the field of view is available for lower heights of sun. It is clear that, for the conditions which these curves represent, the solar altitude should be 30° or less.

The field of view planned for the sensors on the Earth Observatory Satellite is not 100° in angular diameter but half that amount. It is clear from Figure 13 that it would be better to place the field of view off the nadir, away from the sun. For example, the 50° field of view might be chosen to extend from 5° toward the sun to 45° away from the sun. Studies of similar curves for other azimuths and different atmospheric and windspeed conditions seem to make this choice of field of view appear to be wise for many circumstances.

Not all fair weather is as clear as was the day represented by Figures 13 and 14. A more common, hazier, blue-sky occasion was measured near San Diego on 30 July 1964. It is represented by Figures 15 and 16. There was a stable maritime polar air-mass over the sea that day and the sky contained 0.2 to 0.3 broken clouds. The "visibility" was officially reported as 10 miles. The sea-level temperature was 71° to 73°F. and the relative humidity was 60 to 68 percent. Although the sky was blue overhead the horizon appeared gray because of low-level atmospheric haze.

Figure 15 shows that the 560 nm optical signal reaching orbital altitude from an ocean chlorophyll concentration of 0.3 mg/m^3 was virtually undetectable on the "hazy" day just described. Only in a tiny region just below the center of the diagram is there a small part of the field of view in which the sensor can perform its task successfully. This is too small a field to be very useful. That is not to say that the sensor is useless on this occasion. It is merely unable to detect a low

chlorophyll-A pigment concentration that is only three times greater than the arid water threshold. Figure 16, on the other hand, shows that the same sensor can detect a concentration of 0.7 mg/m^3 throughout the entire field of view under these conditions.

Figures 13 through 17 relate to chlorophyll detection by means of green light at 560 nm. Figure 9 shows, however, that in terms of the sub-surface reflectance of ocean water the magnitude of the optical signal for a given chlorophyll-A pigment concentration is greater in the blue region of the spectrum than it is in the green. Scattering of light by the atmosphere, on the other hand, ordinarily attenuates the blue optical signal to a greater extent than it does the green. There has been considerable speculation, therefore, concerning whether the blue signal can be used at orbital altitudes. One result of our study is that on both the clear and the hazy days the blue signal at orbit was greater than the green signal. Even on the hazy day the blue signal was, on the average, 40 percent greater than the green signal. This is illustrated by Figures 17 and 18. The former shows signal contour for green light, a chlorophyll-A pigment concentration of 0.3 mg/m^3, the hazy day, a wind speed of 14 knots when the sea is sprinkled with whitecaps, and a solar zenith angle of 32.4°. Under these circumstances an optical sensor having a threshold at 0.001 will detect the chlorophyll in only two tiny areas near the nadir. Almost the entire field of view is denied to the sensor in terms of green light. Figure 18, however, shows that under essentially identical conditions a blue sensor having the same contrast threshold can perform the detection throughout the entire field of view.

Orbital remote sensors should measure the apparent spectral radiance of the ocean surface throughout most of the visible spectrum in order to differentiate the presence of chlorophyll from other ocean colorants. Any scattering material, such as suspended sediments, can cause the reflectance of the ocean to increase. Therefore, a sensor operating only in terms of 560 nm green light would have no way to distinguish between the presence of sediment and the presence of chlorophyll. Correspondingly, a blue sensor operating only at 450 nm can not distinguish between chlorophyll and other blue-absorbing substances in ocean water. It is probable, however, that only ocean phytoplankton cause the sub-surface reflectance to rise at 560 nm, remain fixed at 523 nm, and diminish at 450 nm. That unique spectral signature is detectable at orbital altitude on the clear and hazy days to which this study applies.

REFERENCES

1. J. E. Tyler and R. C. Smith, Measurements of Spectral Irradiance Underwater (Gordon and Breach Science Publishers, New York, 1970).

2. S. Q. Duntley, J. Opt. Soc. Am. 32, 61 (1942).

3. A. C. Hardy, J. Opt. Soc. Am. 25, 305 (1935).

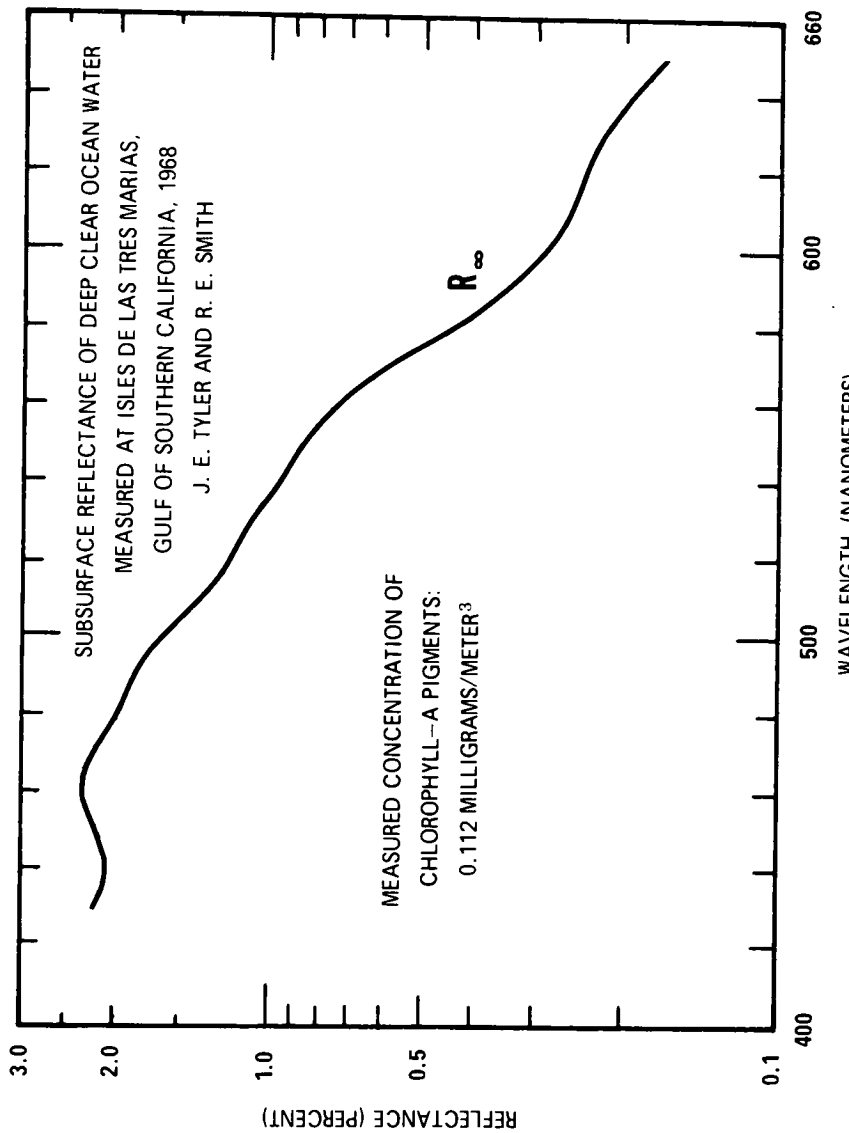
SUBSURFACE REFLECTANCE OF DEEP CLEAR OCEAN WATER
MEASURED AT ISLES DE LAS TRES MARIAS,
GULF OF SOUTHERN CALIFORNIA, 1968
J. E. TYLER AND R. E. SMITH
MEASURED CONCENTRATION OF
CHLOROPHYLL–A PIGMENTS:
0.112 MILLIGRAMS/METER³
R_∞
REFLECTANCE (PERCENT)
3.0
2.0
1.0
0.5
0.1
400
500
600
660
WAVELENGTH (NANOMETERS)

Figure 1

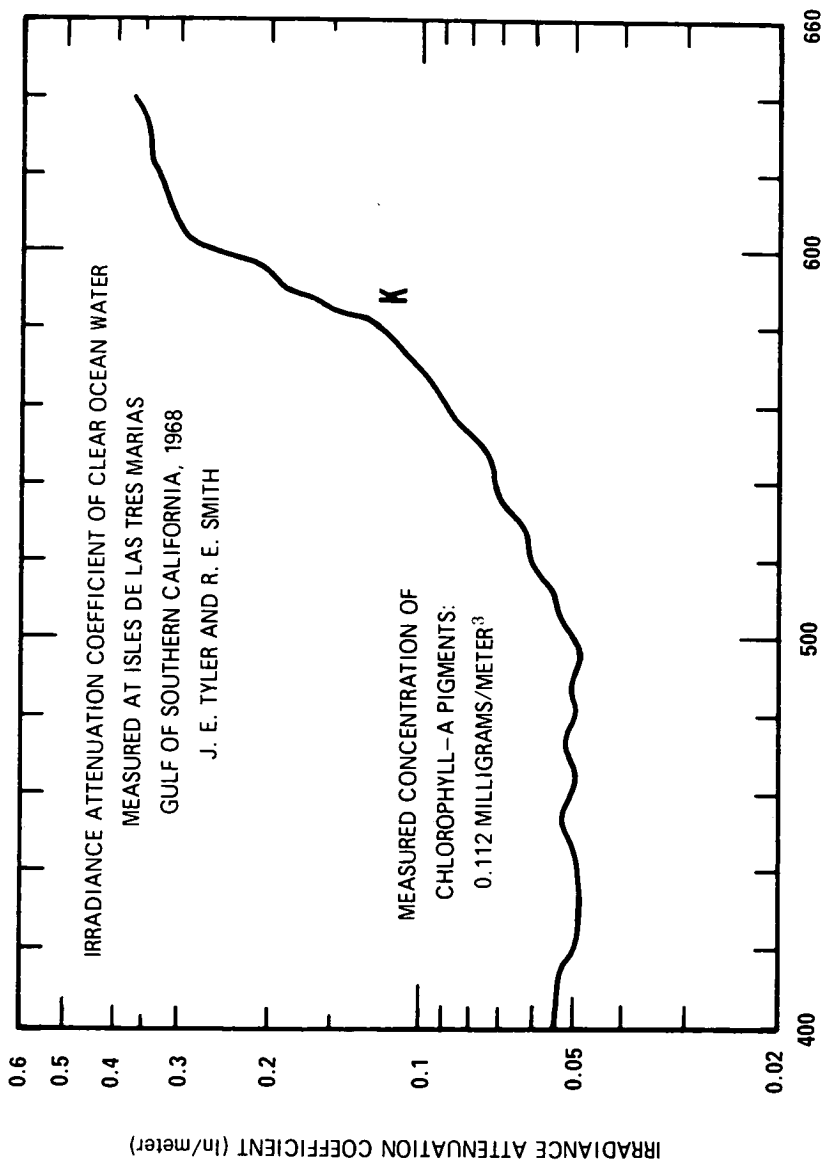
IRRADIANCE ATTENUATION COEFFICIENT OF CLEAR OCEAN WATER
MEASURED AT ISLES DE LAS TRES MARIAS
GULF OF SOUTHERN CALIFORNIA, 1968
J. E. TYLER AND R. E. SMITH
MEASURED CONCENTRATION OF
CHLOROPHYLL-A PIGMENTS:
0.112 MILLIGRAMS/METER3
K
IRRADIANCE ATTENUATION COEFFICIENT (In/meter)
0.6
0.5
0.4
0.3
0.2
0.1
0.05
0.02
400
500
600
660
WAVELENGTH (NANOMETERS)

Figure 2

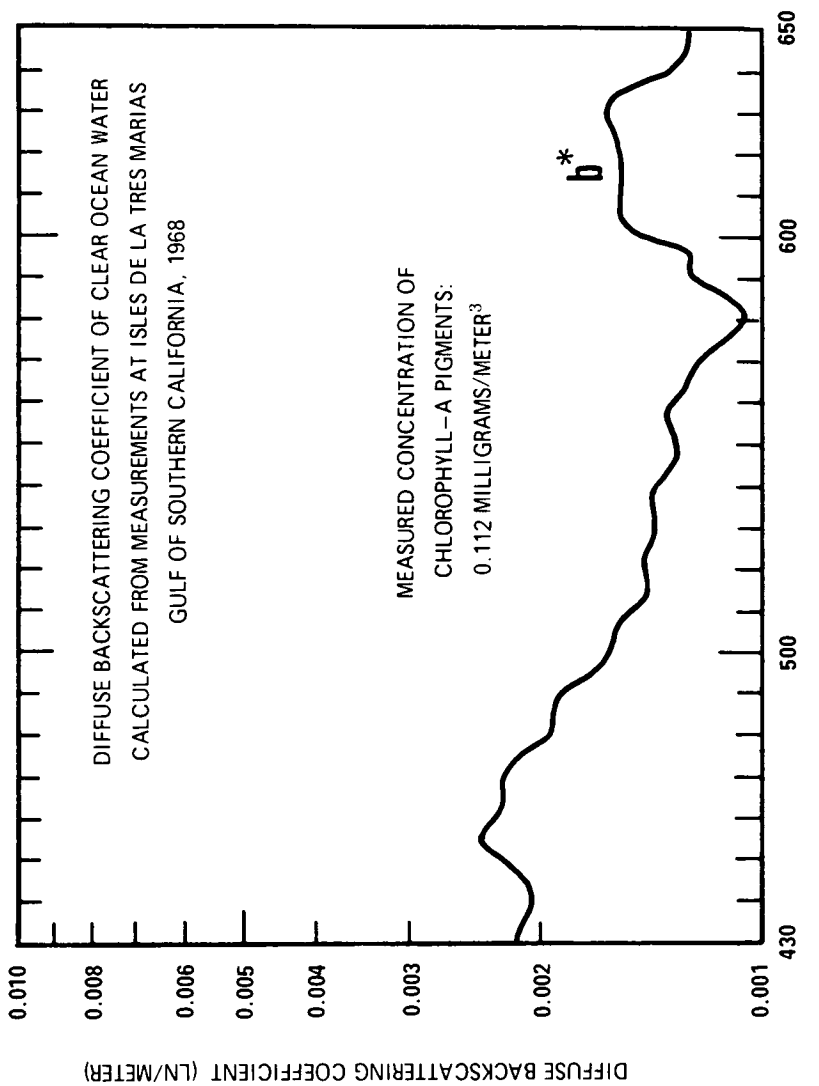
DIFFUSE BACKSCATTERING COEFFICIENT OF CLEAR OCEAN WATER
CALCULATED FROM MEASUREMENTS AT ISLES DE LA TRES MARIAS
GULF OF SOUTHERN CALIFORNIA, 1968
MEASURED CONCENTRATION OF
CHLOROPHYLL-A PIGMENTS:
0.112 MILLIGRAMS/METER3
b*
DIFFUSE BACKSCATTERING COEFFICIENT (LN/METER)
0.010
0.008
0.006
0.005
0.004
0.003
0.002
0.001
430
500
600
650
WAVELENGTH (NANOMETERS)

Figure 3

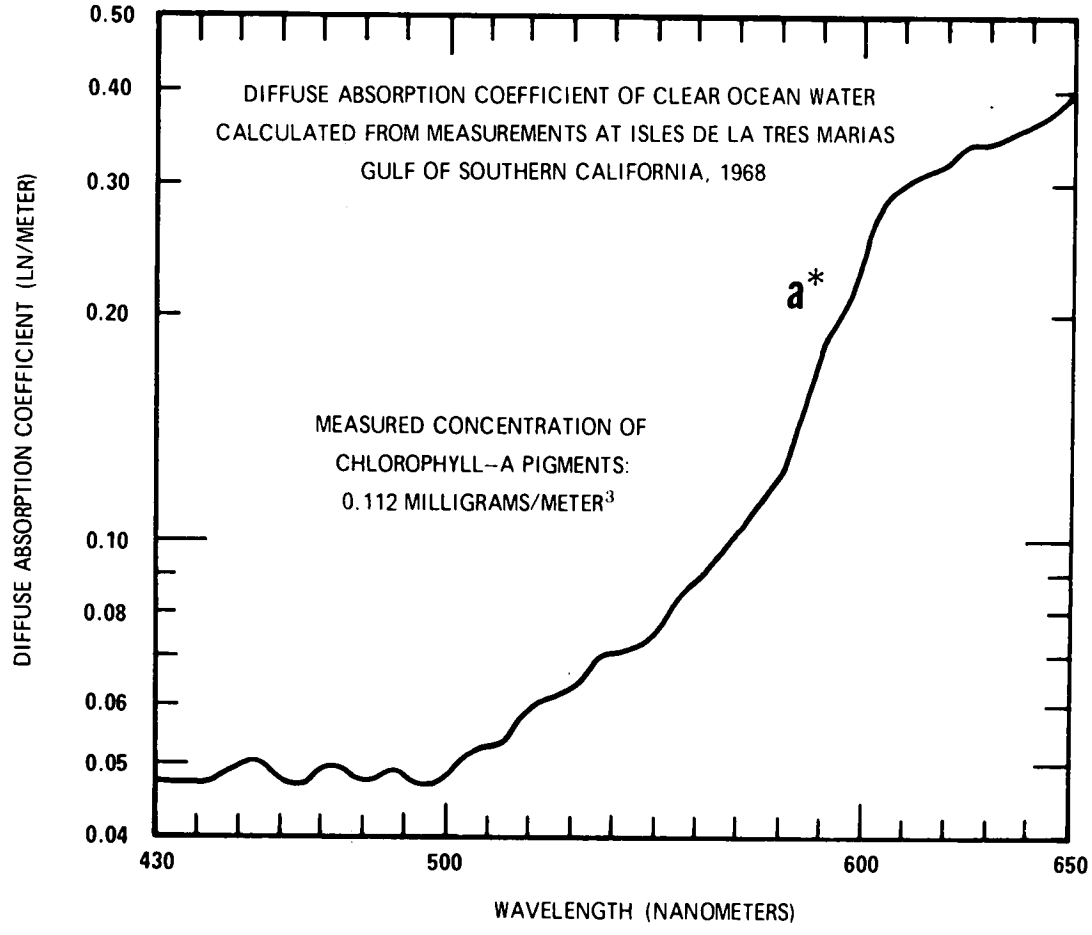
DIFFUSE ABSORPTION COEFFICIENT OF CLEAR OCEAN WATER
CALCULATED FROM MEASUREMENTS AT ISLES DE LA TRES MARIAS
GULF OF SOUTHERN CALIFORNIA, 1968
a*
MEASURED CONCENTRATION OF
CHLOROPHYLL–A PIGMENTS:
0.112 MILLIGRAMS/METER3
DIFFUSE ABSORPTION COEFFICIENT (LN/METER)
0.50
0.40
0.30
0.20
0.10
0.08
0.06
0.05
0.04
430
500
600
650
WAVELENGTH (NANOMETERS)

Figure 4

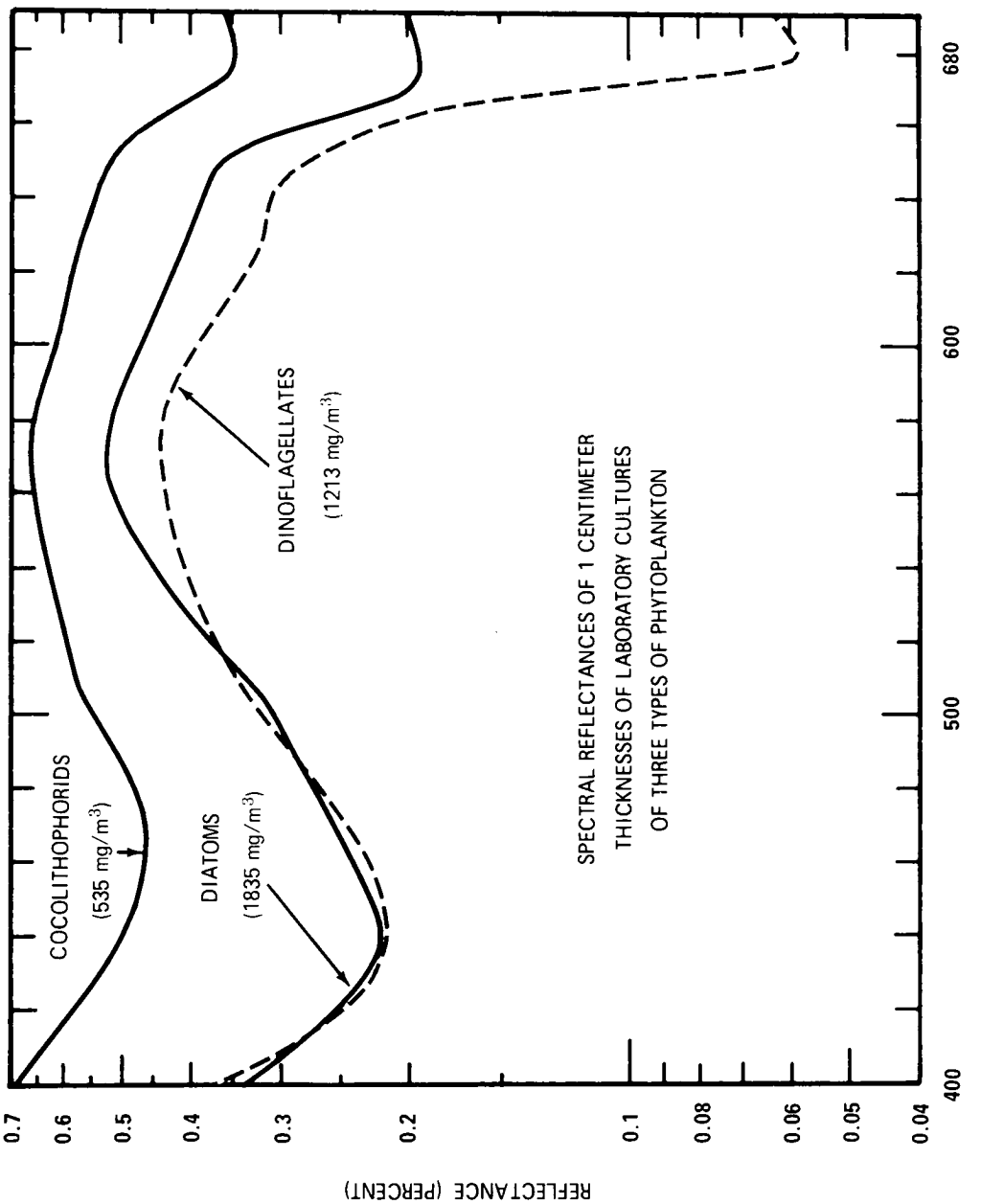
COCOLITHOPHORIDS
(535 mg/m³)
DIATOMS
(1835 mg/m³)
DINOFLAGELLATES
(1213 mg/m³)
SPECTRAL REFLECTANCES OF 1 CENTIMETER
THICKNESSES OF LABORATORY CULTURES
OF THREE TYPES OF PHYTOPLANKTON
REFLECTANCE (PERCENT)
0.7
0.6
0.5
0.4
0.3
0.2
0.1
0.08
0.06
0.05
0.04
400
500
600
680
WAVELENGTH (NANOMETERS)

Figure 5

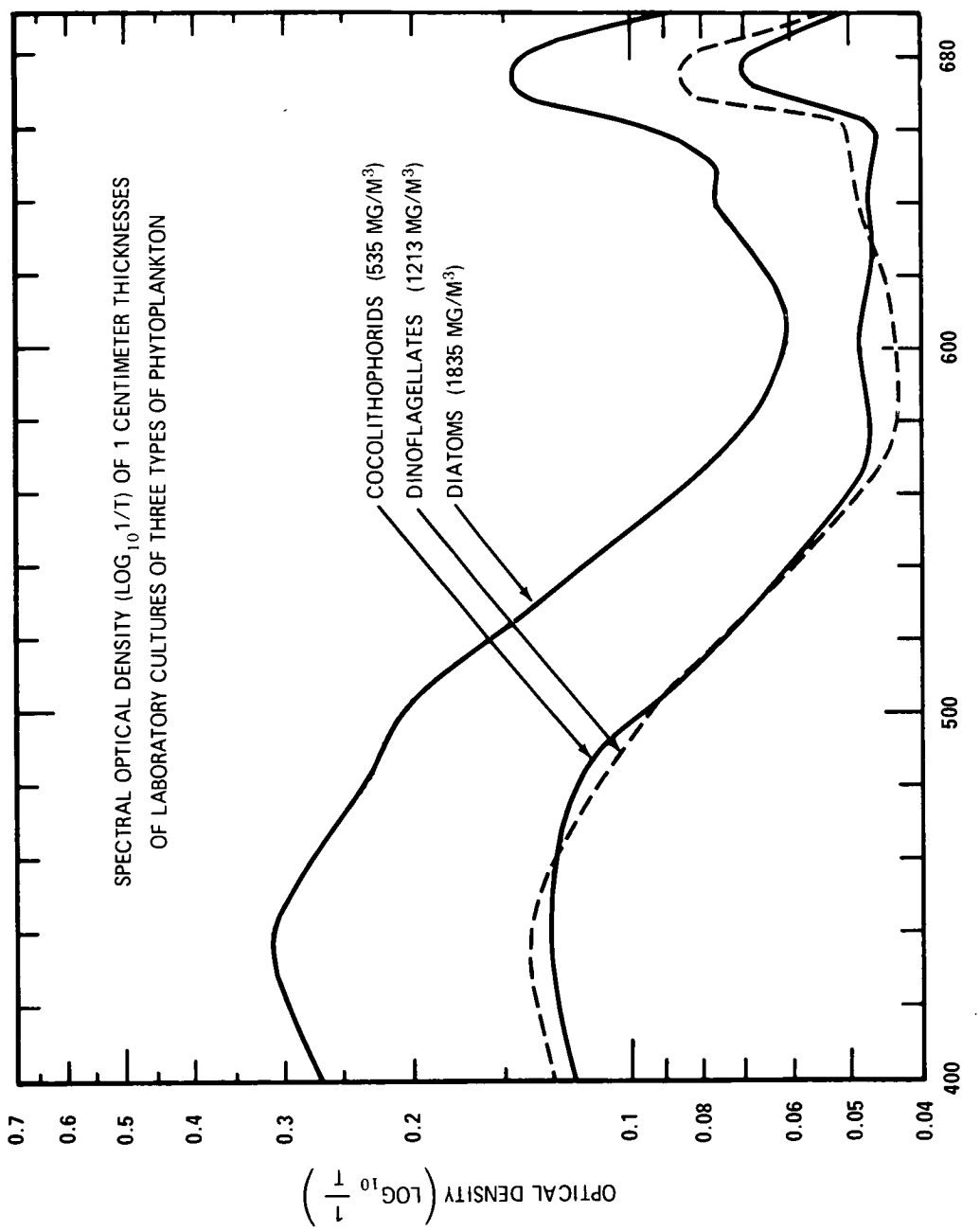
SPECTRAL OPTICAL DENSITY ($LOG_{10}1/T$) OF 1 CENTIMETER THICKNESSES
OF LABORATORY CULTURES OF THREE TYPES OF PHYTOPLANKTON
COCOLITHOPHORIDS (535 MG/M^3)
DINOFLAGELLATES (1213 MG/M^3)
DIATOMS (1835 MG/M^3)
OPTICAL DENSITY $\left(LOG_{10}\frac{1}{T}\right)$
0.7
0.6
0.5
0.4
0.3
0.2
0.1
0.08
0.06
0.05
0.04
400
500
600
680
WAVELENGTH (NANOMETERS)

Figure 6

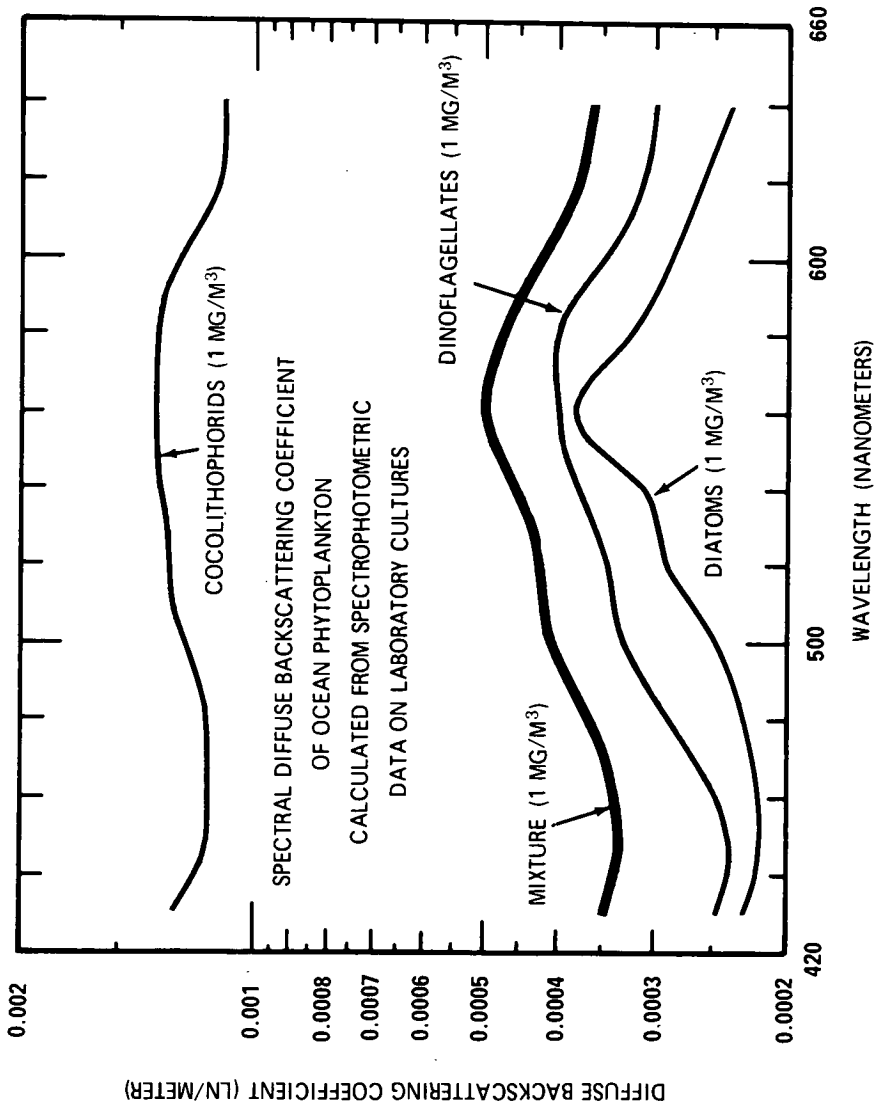
SPECTRAL DIFFUSE BACKSCATTERING COEFFICIENT
OF OCEAN PHYTOPLANKTON
CALCULATED FROM SPECTROPHOTOMETRIC
DATA ON LABORATORY CULTURES
COCOLITHOPHORIDS (1 MG/M3)
DINOFLAGELLATES (1 MG/M3)
MIXTURE (1 MG/M3)
DIATOMS (1 MG/M3)
DIFFUSE BACKSCATTERING COEFFICIENT (LN/METER)
0.002
0.001
0.0008
0.0007
0.0006
0.0005
0.0004
0.0003
0.0002
420
500
600
660
WAVELENGTH (NANOMETERS)

Figure 7

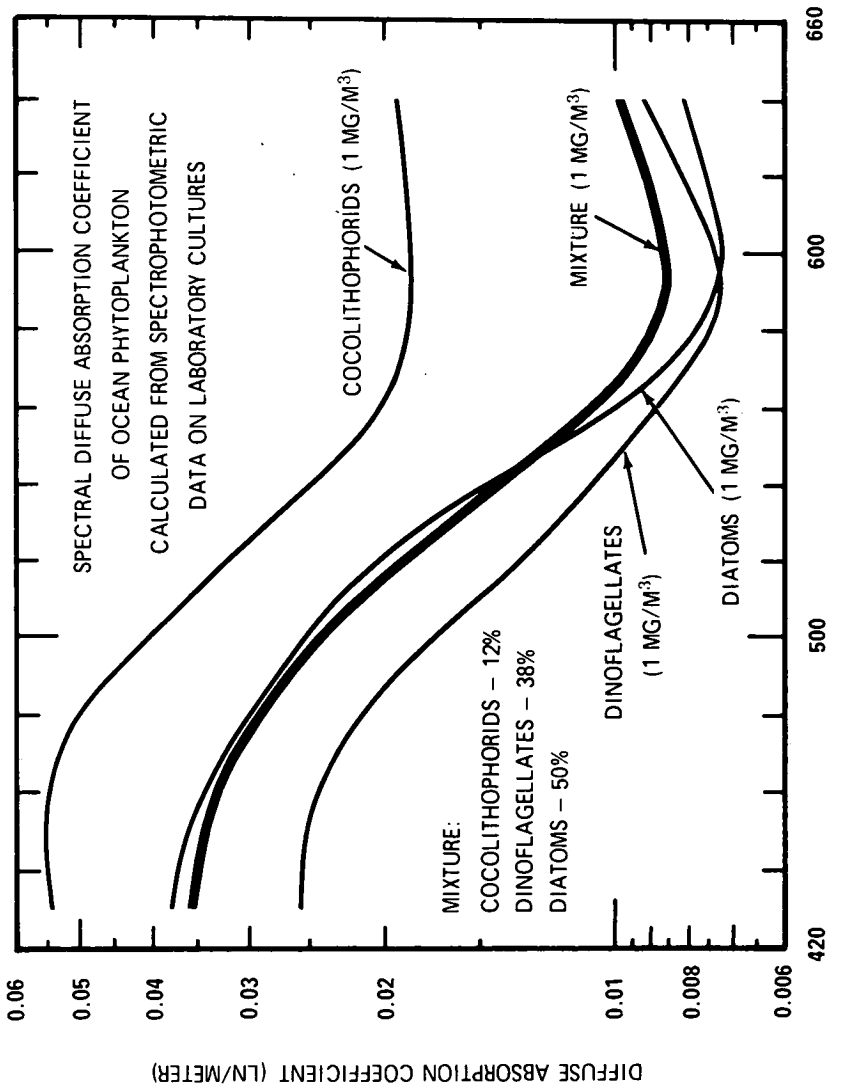
SPECTRAL DIFFUSE ABSORPTION COEFFICIENT
OF OCEAN PHYTOPLANKTON
CALCULATED FROM SPECTROPHOTOMETRIC
DATA ON LABORATORY CULTURES
COCOLITHOPHORIDS (1 MG/M3)
MIXTURE (1 MG/M3)
DINOFLAGELLATES
(1 MG/M3)
DIATOMS (1 MG/M3)
MIXTURE:
COCOLITHOPHORIDS – 12%
DINOFLAGELLATES – 38%
DIATOMS – 50%
0.06
0.05
0.04
0.03
0.02
0.01
0.008
0.006
420
500
600
660
DIFFUSE ABSORPTION COEFFICIENT (LN/METER)
WAVELENGTH (NANOMETERS)

Figure 8

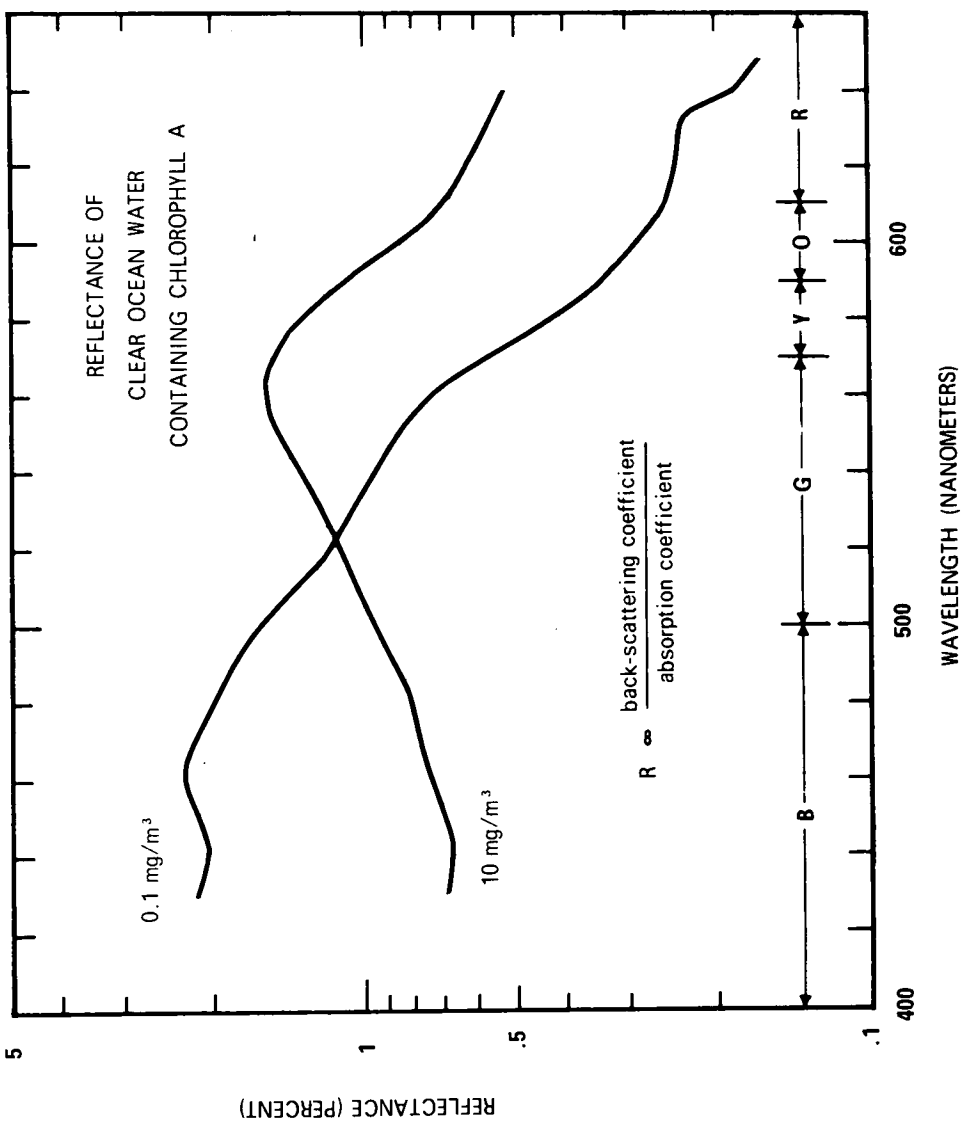
REFLECTANCE OF
CLEAR OCEAN WATER
CONTAINING CHLOROPHYLL A
0.1 mg/m³
10 mg/m³
R ∞ back-scattering coefficient / absorption coefficient
B
G
Y
O
R
5
1
.5
.1
400
500
600
WAVELENGTH (NANOMETERS)
REFLECTANCE (PERCENT)

Figure 9

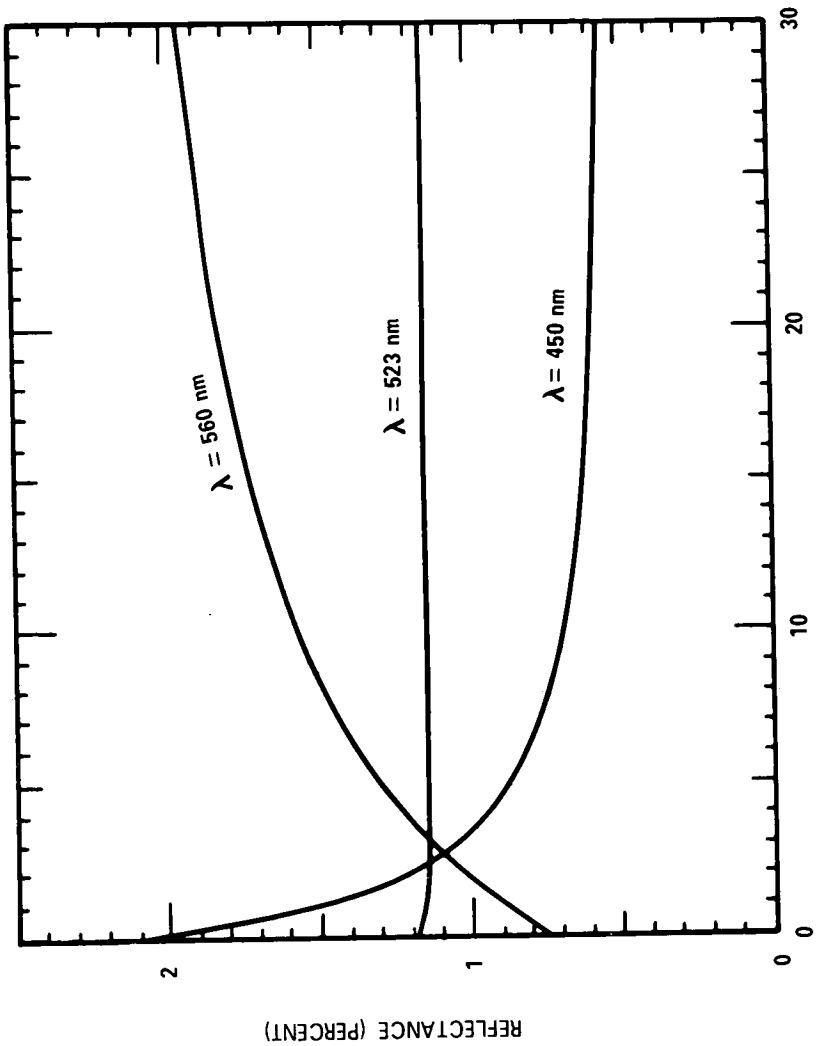
λ = 560 nm
λ = 523 nm
λ = 450 nm
REFLECTANCE (PERCENT)
0
1
2
0
10
20
30
CONCENTRATION OF CHLOROPHYLL-A PIGMENTS IN CLEAR OCEAN WATER
(MILLIGRAMS/METER^3)

Figure 10

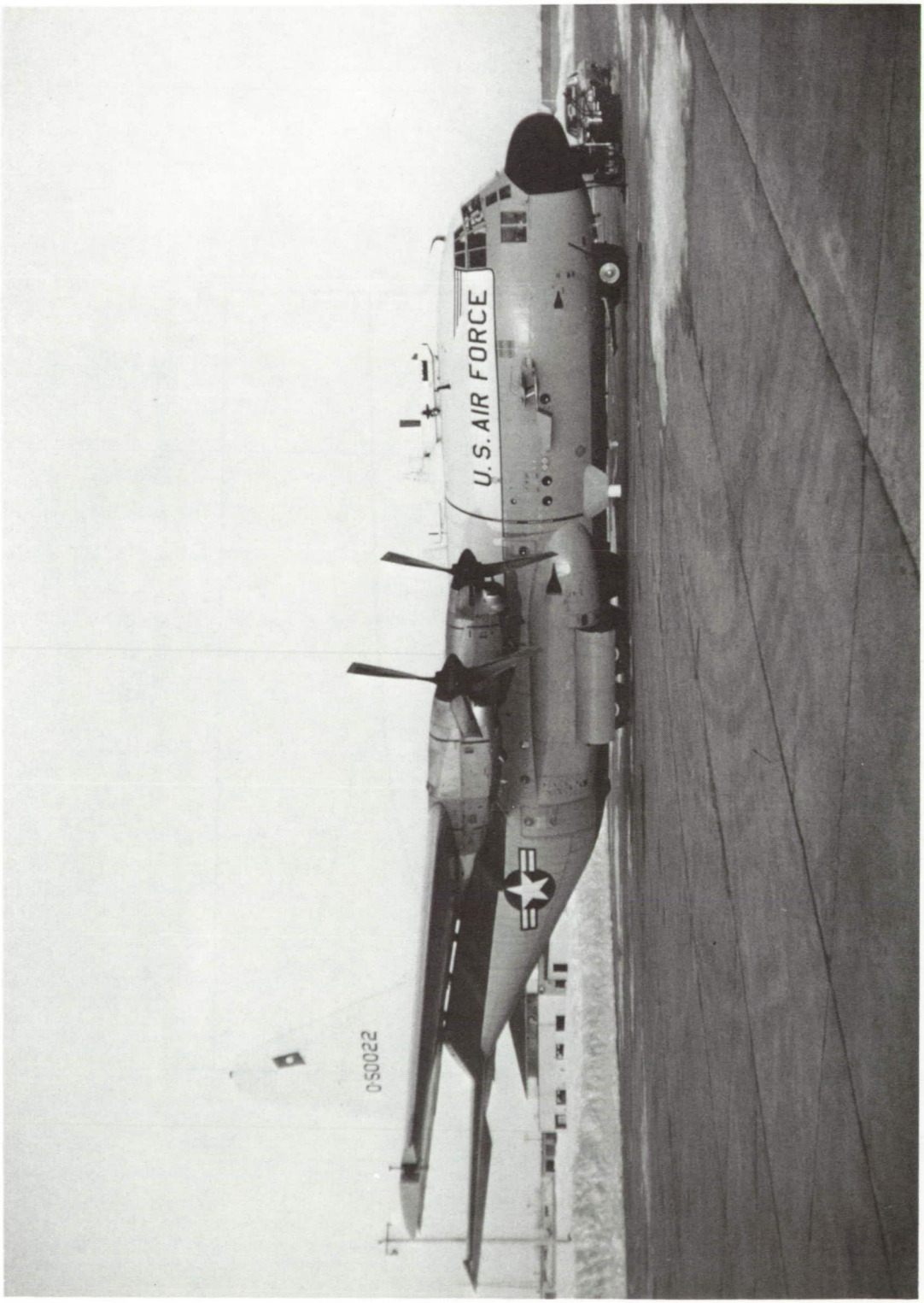

Figure 11. Instrumented C-130 Aircraft

Figure 12. Contrast Reduction Meter

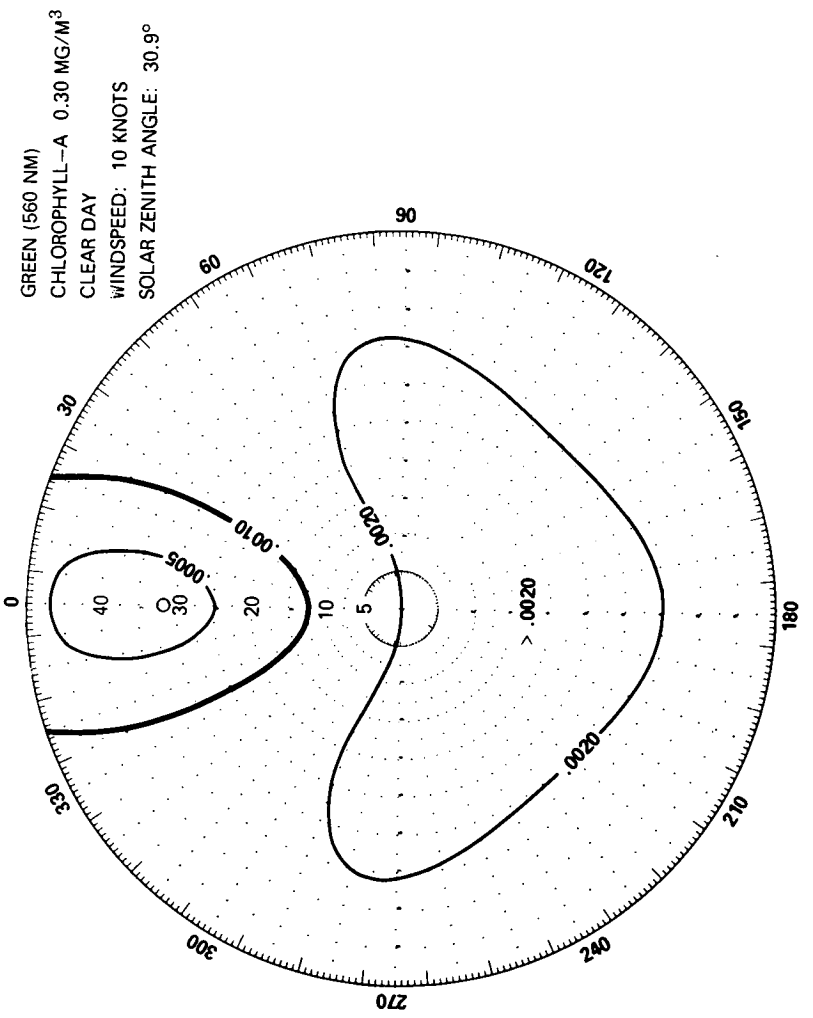
GREEN (560 NM)
CHLOROPHYLL-A 0.30 MG/M3
CLEAR DAY
WINDSPEED: 10 KNOTS
SOLAR ZENITH ANGLE: 30.9°
0
30
60
90
120
150
180
210
240
270
300
330
40
30
20
10
5
.0005
.0010
.0020
.0020
> .0020

Figure 13

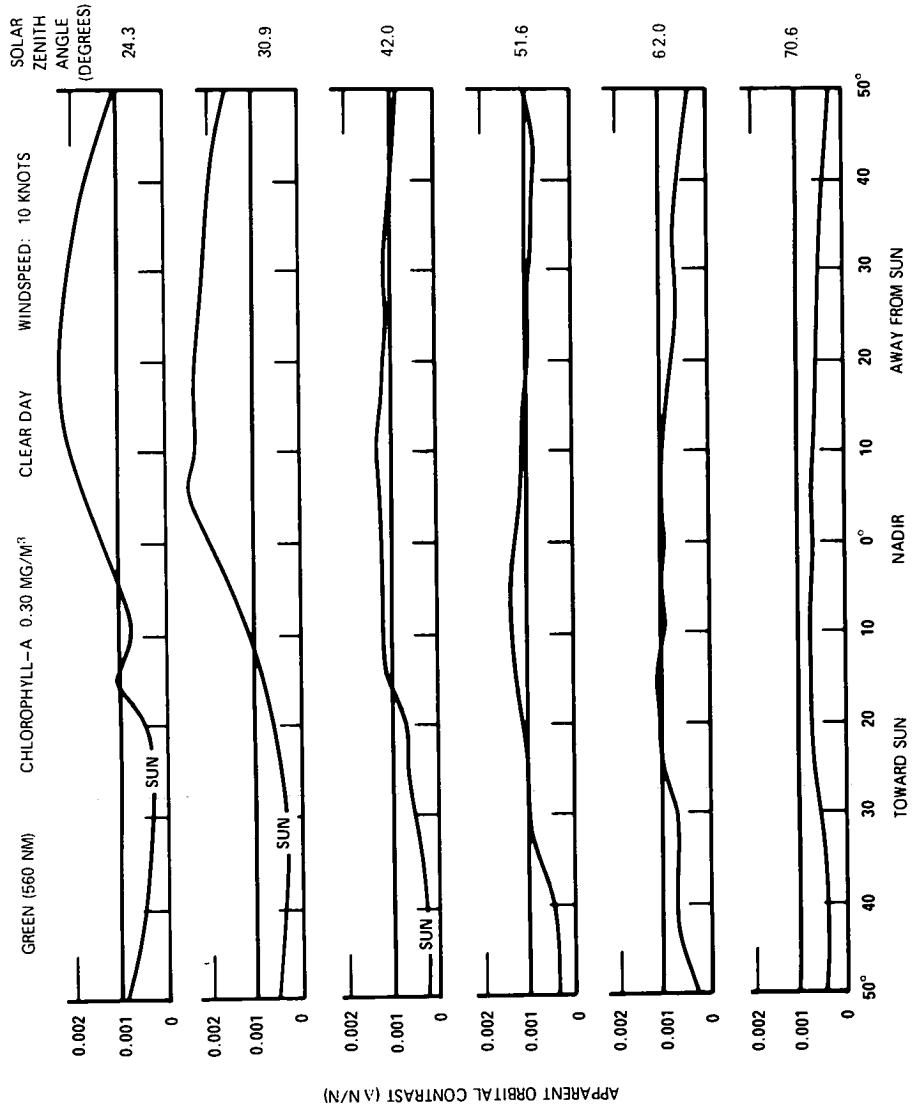
GREEN (560 NM) CHLOROPHYLL-A 0.30 MG/M³ CLEAR DAY WINDSPEED: 10 KNOTS
SOLAR ZENITH ANGLE (DEGREES)
24.3
30.9
42.0
51.6
62.0
70.6
SUN
0.002
0.001
0
APPARENT ORBITAL CONTRAST (ΔN/N)
50°
40
30
20
10
0°
TOWARD SUN
NADIR
AWAY FROM SUN

Figure 14

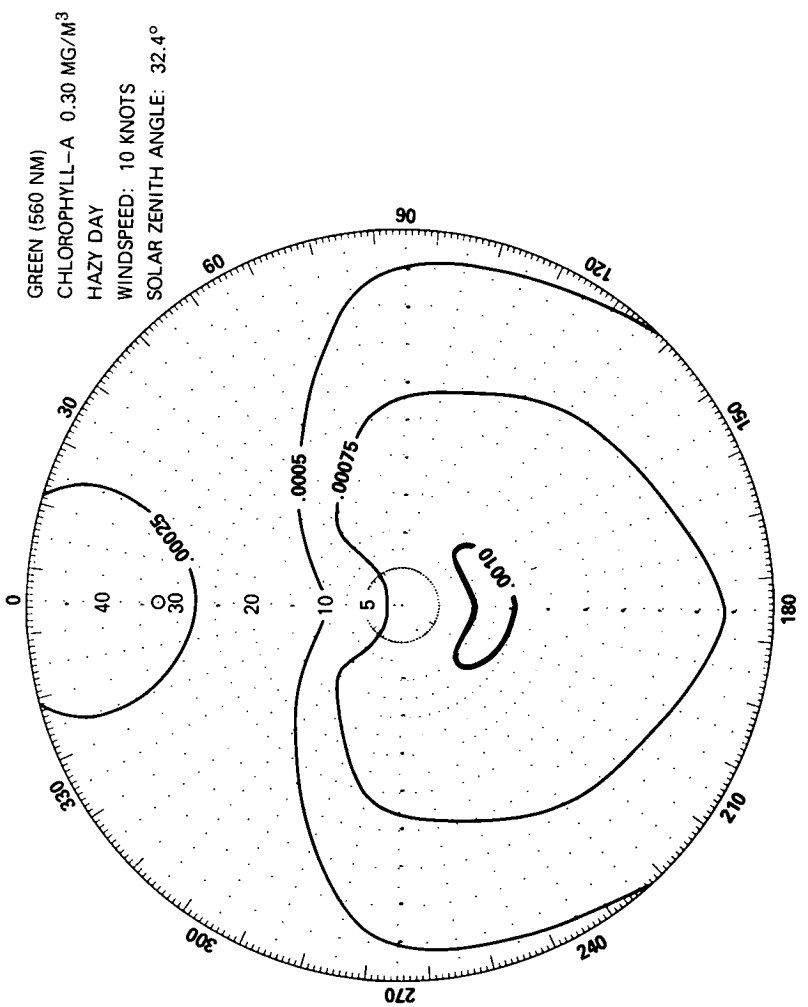
GREEN (560 NM)
CHLOROPHYLL-A 0.30 MG/M3
HAZY DAY
WINDSPEED: 10 KNOTS
SOLAR ZENITH ANGLE: 32.4°
0
30
60
90
120
150
180
210
240
270
300
330
40
30
20
10
5
.00025
.0005
.00075
.0010

Figure 15

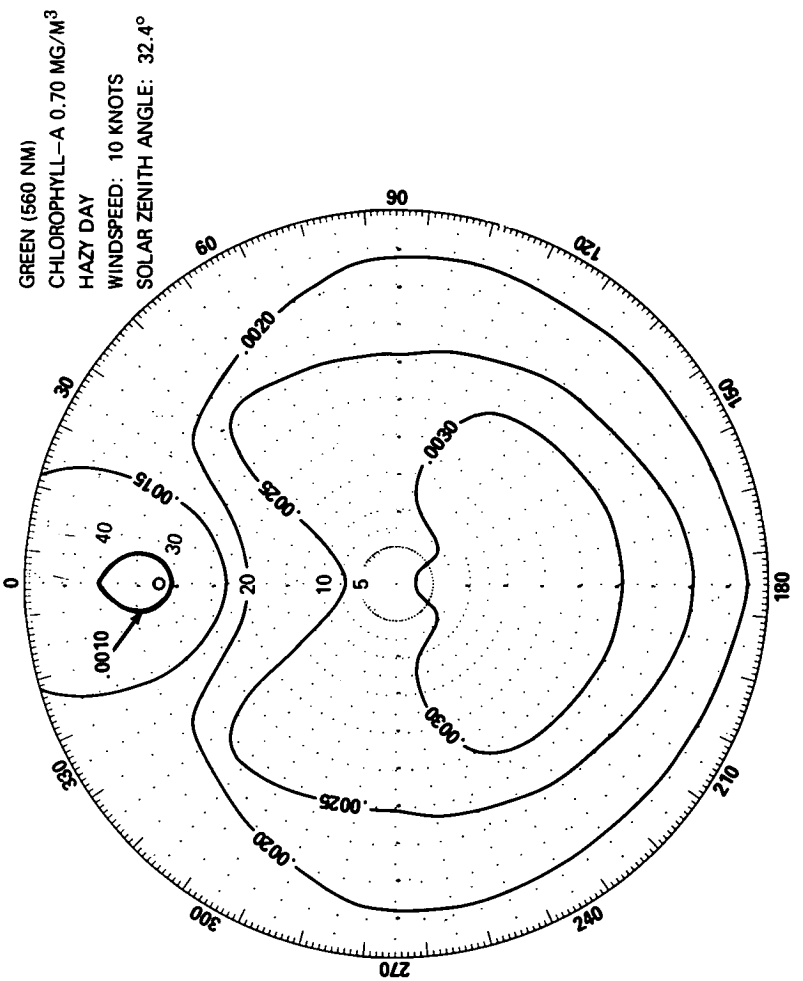
GREEN (560 NM)
CHLOROPHYLL–A 0.70 MG/M3
HAZY DAY
WINDSPEED: 10 KNOTS
SOLAR ZENITH ANGLE: 32.4°
0
30
60
90
120
150
180
210
240
270
300
330
.0010
.0015
.0020
.0025
.0030
40
30
20
10
5

Figure 16

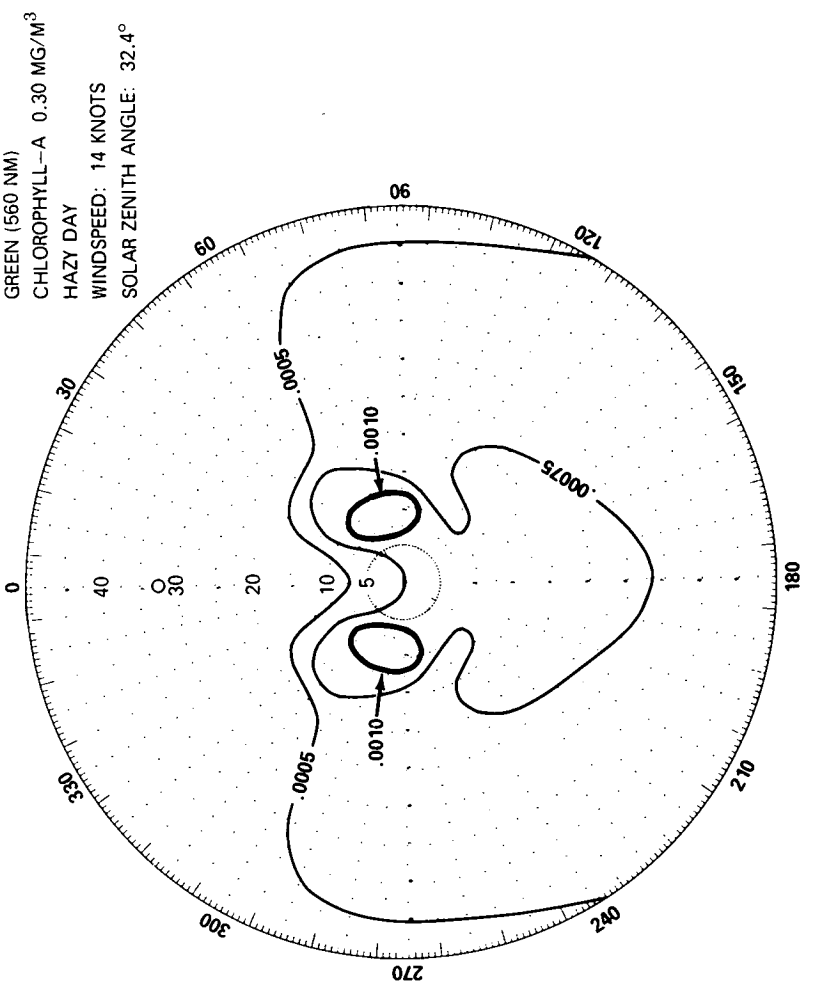
GREEN (560 NM)
CHLOROPHYLL-A 0.30 MG/M3
HAZY DAY
WINDSPEED: 14 KNOTS
SOLAR ZENITH ANGLE: 32.4°
0
30
60
90
120
150
180
210
240
270
300
330
40
30
20
10
5
.0005
.0010
.00075
.0005
.0010

Figure 17

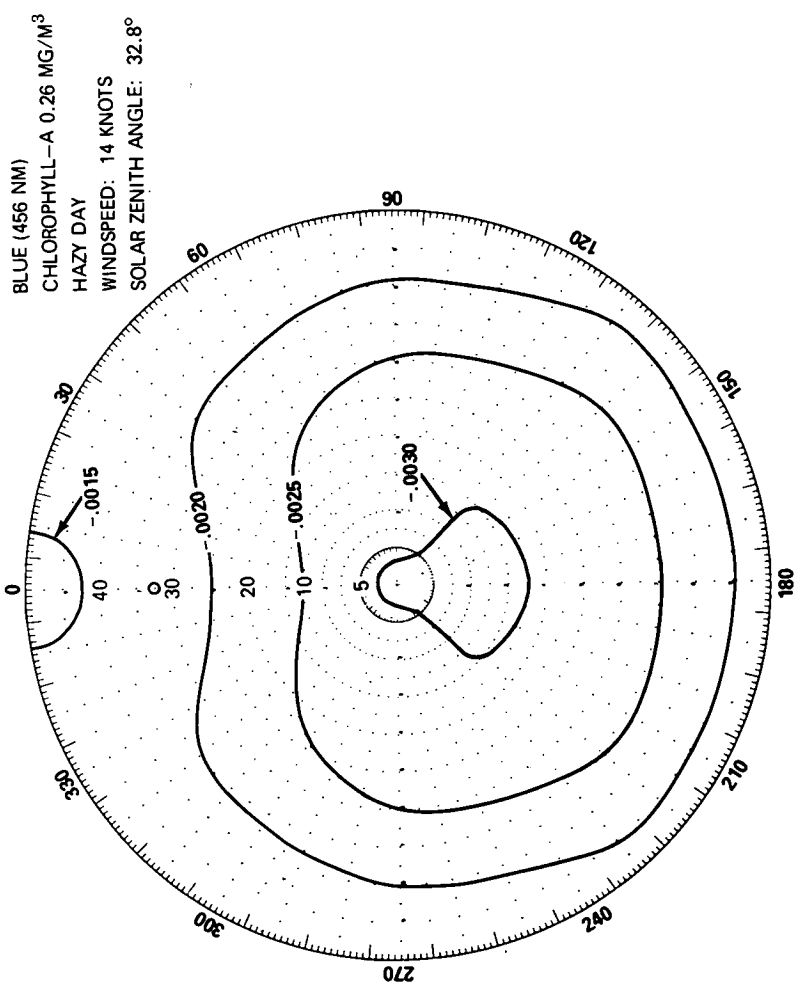
BLUE (456 NM)
CHLOROPHYLL–A 0.26 MG/M3
HAZY DAY
WINDSPEED: 14 KNOTS
SOLAR ZENITH ANGLE: 32.8°
0
30
60
90
120
150
180
210
240
270
300
330
-.0015
-.0020
-.0025
-.0030
40
30
20
10
5

Figure 18